energies

MDPI

Article

Retrofit of Diesel Engines with H_2 for Potential Decarbonization of Non-Electrified Railways: Assessment with Lifecycle Analysis and Advanced Numerical Modeling

Mehrshad Kolahchian Tabrizi, Tarcisio Cerri, Davide Bonalumi *, Tommaso Lucchini and Morris Brenna

Department of Energy, Politecnico di Milano, Via Lambruschini 4, 20156 Milano, Italy; mehrshad.kolahchian@polimi.it (M.K.T.); tarcisio.cerri@sursum-mi.com (T.C.); tommaso.lucchini@polimi.it (T.L.); morris.brenna@polimi.it (M.B.)

* Correspondence: davide.bonalumi@polimi.it; Tel.: +39-02-2399-3817

Abstract: The application of hydrogen in heavy-duty vehicles or trains has been suggested as a promising solution to decarbonize the transportation sector. In this study, a one-dimensional engine modeling is employed to evaluate the potential of hydrogen as a fuel for railway applications. A turbocharged diesel engine is simulated as the baseline unit, and the results are validated with experimental data. The same engine is converted to become compatible with hydrogen through some modifications in the turbocharger group and the injection and ignition systems to preserve the performance of the baseline configuration. The findings show that the engine traction power is reduced from 600 to 400 kW, indicating an inferior performance for the hydrogen-fueled engine. The energy consumption of the hydrogen-fueled engine on a real train mission profile is almost two times the diesel version. However, our Life Cycle Assessment analysis with a Well-to-Wheel system boundary shows a 56% reduction in equivalent CO_2 emissions for the engine fueled with photovoltaic-based green hydrogen. Substituting diesel with low-carbon hydrogen can decrease the train's carbon footprint from 4.27 to even less than 2 kg CO_2 eq./km, suggesting that moderately modified engines are a promising solution for decarbonizing non-feasibly electrified railway sections.

Keywords: hydrogen; trains; Life Cycle Assessment; transportation; green hydrogen; carbon footprint

Citation: Kolahchian Tabrizi, M.; Cerri, T.; Bonalumi, D.; Lucchini, T.; Brenna, M. Retrofit of Diesel Engines with H_2 for Potential Decarbonization of Non-Electrified Railways: Assessment with Lifecycle Analysis and Advanced Numerical Modeling. *Energies* **2024**, *17*, 996. https://doi.org/10.3390/en17050996

Academic Editors: Davide Lanni and Enzo Galloni

Received: 16 January 2024
Revised: 6 February 2024
Accepted: 8 February 2024
Published: 20 February 2024

1. Introduction

Hydrogen is becoming a potential solution for decarbonizing energy systems. According to net-zero emission (NZE) scenarios, hydrogen and H_2-based fuels will account for 10% of total final energy consumption in 2050 [1]. New applications like hard-to-abate industries, power generation, and transport will constitute 40% of the H_2 demand in 2030 [2]. For vehicles, the application of lithium-ion batteries in electric vehicles can be promising, specifically for smaller vehicles circulating in countries with lower electricity carbon intensity [3,4]. However, for decarbonizing heavy-duty vehicles or trains, hydrogen can become a more appropriate solution [5–7]. On the one hand, there has been a growing interest in introducing fuel cell-based hydrogen trains for use on railway lines that cannot be or are not conveniently electrified due to geometric constraints or low traffic characterizations [8,9]. On the other hand, many newly built diesel train fleets could benefit from the conversion of their internal combustion engine (ICE) to become compatible with hydrogen fuel, reducing their environmental impact with limited costs [10,11].

Hydrogen can be obtained using a wide range of methodologies, of which some of them can produce hydrogen with low environmental impacts, notably low CO_2 equivalent emissions. In 2022, only less than 1% of the produced hydrogen (less than 9.5 Mt) was obtained via a low-carbon route; however, the low-carbon H_2 production is expected to reach 450 Mt in 2050 [2]. High Technology Readiness Level (TRL) and the possibility of scaling up the production made the water electrolysis powered by renewable electricity

(Green H_2) and reforming of fossil fuels coupled with carbon capture, utilization, and storage (Blue H_2) the main routes for low-carbon H_2 production. Based on the NZE scenario defined by the International Energy Agency (IEA), by 2030, 40% of electricity will be generated by photovoltaic (PV) and wind sources with a subsequent increase to 70% by 2050 [1]. Therefore, wind and PV electricity will become the main power sources for electrolysis systems.

Life Cycle Assessment (LCA) can be employed to calculate the environmental impacts associated with products or services. Similarly, LCA can be applied to compute the carbon footprint of different H_2 production methods. Within an LCA analysis, a Well-to-Wheel system boundary can be used to compare the environmental performance of various fuels used for transportation purposes.

This work aims to evaluate the potential of hydrogen-fueled internal combustion engines for railway applications, featuring an LCA analysis to investigate the carbon footprint of these trains. Particularly, the study focuses on Diesel Multiple Units (DMUs) with electric traction motors, which are already in operation on non-electrified lines in several European countries. The diesel engine configuration is considered as a baseline. Numerical one-dimensional simulations using the Gasdyn code 2022 [12–16] are employed to estimate the fuel consumption of diesel or hydrogen-fueled railway vehicles on a real train mission profile. The simulation results for the diesel engine are validated with experimental data on power and fuel consumption in the operating points relevant to the train operation. The diesel engine unit is moderately converted to become compatible with hydrogen. The modifications are limited to the replacement of the combustion and injection systems and the turbocharger group to restrict the cost burdens. Finally, the climate profile of the baseline diesel train and the hydrogen-fueled train are analyzed.

2. Materials and Methods

In this section, the performance of the original diesel engine train is defined in Section 2.1. The methodology adopted for the conversion of diesel-based engines to hydrogen-fueled is explained in Section 2.2. The application of Life Cycle Assessment with the Well-to-Wheel system boundary is described in Section 2.3.

2.1. Performance of the Original Railway Vehicle

The investigated configuration consists of a single-decker articulated railway vehicle (also known as DMU—Diesel Multiple Unit) equipped with two identical diesel engines. Tables 1 and 2 summarize the main technical data of the vehicle and engine, respectively.

Table 1. Main characteristics of the railway vehicle under investigation.

Parameter	Description
Diesel engine rated power [kW]	2 × 365
Vehicle mass [kg]	68,000
Vehicle maximum speed [km/h]	140
Maximum power at wheels [kW]	600
Starting tractive force [kN]	80
Maximum acceleration [m/s^2]	1.0

Table 2. Main characteristics of the diesel engine.

Parameter	Description
Engine arrangement [-]	6 in line
Bore [cm]	12.8
Stroke [cm]	16.6
Total displacement [cm^3]	12,816
Compression ratio [-]	18:1
Emission compliance	Tier IIIA

The schematic of the diesel–electric arrangement of the studied DMU is shown in Figure 1. The DMU under study has a diesel–electric arrangement. The power generated by the internal combustion engine is transferred to the wheels by decoupling the torque and speed parameters. In particular, the ICE can deliver constant power while the rotation speed and the delivered torque are kept constant, even as the torque and speed produced by the electric motors connected to the wheels vary.

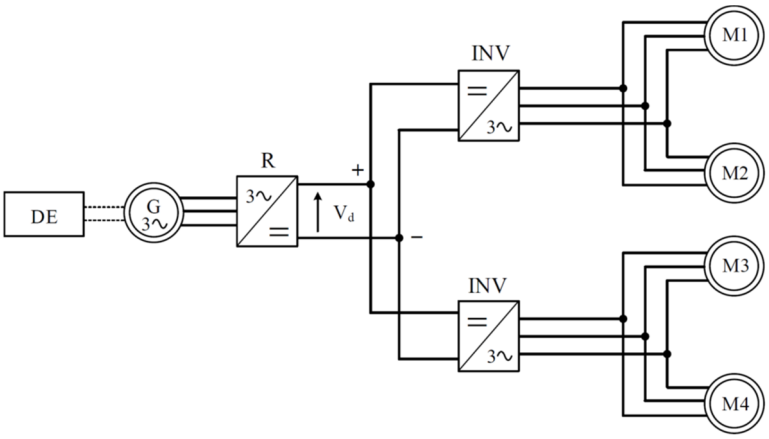

Figure 1. Diesel–electric arrangement for a DMU.

Figure 2 summarizes the performance of the railway vehicle operating with a diesel engine in terms of both maximum tractive force and the corresponding power at wheels as a function of the vehicle velocity. The maximum power supplied by two engines is higher than the one required by the wheels, where the difference is available for the onboard systems (electronic converters, interior lighting, air conditioning, etc.).

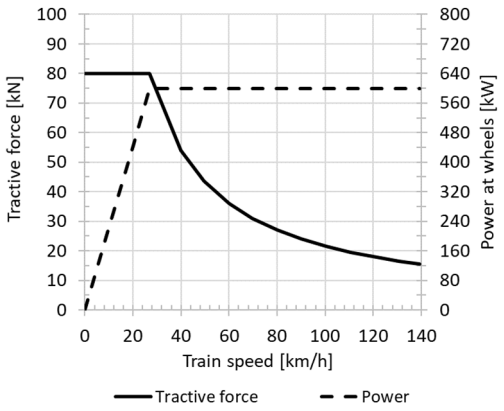

Figure 2. Tractive force (mechanical characteristic) and wheel power as a function of train speed when diesel thermal units work on the train.

Given the required engine constant power (P), the corresponding load (L), the duration for which the engine is switched on (t), and the revolution speed (n) at which power is delivered, it is possible to compute the fuel consumption for a specific mission profile using Equation (1):

$$m_{fuel} = P(n,\ L) \cdot BSFC(n, L) \cdot t_{switched\ on} \quad (1)$$

where *BSFC* is the brake-specific fuel consumption for the corresponding operating point. One-dimensional numerical simulations are used to estimate *BSFC*. The Gasdyn code is employed in this work to simulate the investigated engine operating with diesel and hydrogen fuels. Gasdyn is a one-dimensional thermo-fluid dynamic model continuously developed and enhanced by the researchers at Politecnico di Milano. The main features of the numerical code are described in previous works [10–14]. The model is developed

for the simulation of internal combustion engines coupled with their complete intake and exhaust systems, allowing for a detailed analysis of the fluid dynamic and thermal and chemical behaviors of the entire engine system. The Gasdyn code uses a set of different numerical solvers, including symmetric TVD finite difference techniques with second-order accuracy as described in [17]. Following a characteristic-based approach to the calculation of Riemann variables [18], boundary conditions and intra-pipe connections are developed for the representation of components such as turbochargers, multi-pipe junctions, abrupt area changes, inlet and outlet, etc. [18].

For compression ignition combustion, the model is designed to handle modern multi-pulse injection systems. Within the model, the combustion chamber is subdivided into three zones: fresh charge (air + residual gas), fuel (already vaporized), and burned gas. Pressure is assumed to be constant in the entire combustion chamber, directly ensuring the fulfillment of momentum conservation. Therefore, the solution of the mass and energy equations applied to the burned, unburned, and fuel zones allows for the computation of the pressure and temperature of the three zones. Each discrete injection event during the engine cycle is defined as a pulse, where up to 4 pulses can be considered. The burning rate of a single pulse is expressed as the sum of two stages, one describing the premixed phase and the other describing the diffusive phase. The rate of the burned mass fraction is calculated using the Wiebe equation, applied to the premixed and diffusive combustion processes. Distinct Wiebe coefficients are employed for each pulse (pre1, pre2, main, and post pulses) [19]. The entire engine layout is modeled, including the turbocharger, with a suitable model to predict the in-cylinder pressure development typical of compression ignition combustion.

Regarding the spark ignition combustion of the hydrogen-fueled engine, a two-zone, quasi-dimensional combustion model is used to predict the in-cylinder pressure development. The Zimont model [20] is employed to compute the fully developed turbulent flame speed, enabling the [20] evaluation of thermodynamic and chemical gas properties inside the combustion chamber [14,16]. In both combustion models, the heat transfer coefficient between the gas inside the cylinder and cylinder walls is calculated using the Woschni correlation [21].

Figure 3 compares the measured and predicted power and BSFC of the diesel engine configuration at full-load conditions. The operating point of the mounted thermal engine on DMU is specified at 1500 rpm. The predicted and estimated values are in good agreement. This alignment suggests that the proposed numerical approach can be used for a realistic estimation of diesel fuel consumption across different mission profiles.

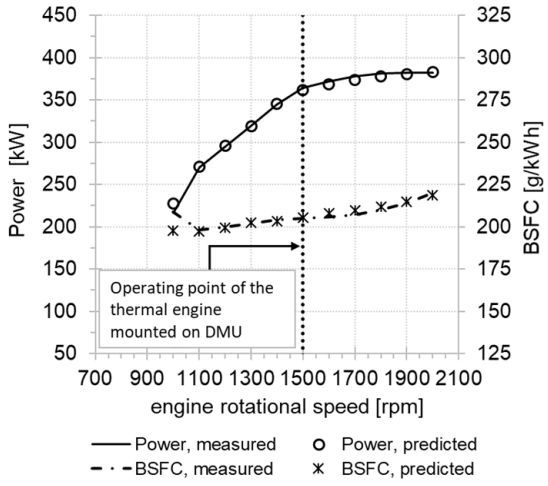

Figure 3. Comparison between measured and predicted performance of the diesel engine at full load conditions (the operating point of the thermal engine mounted on DMU is specified).

2.2. Engine Conversion to Hydrogen Fuel

The diesel engine unit is modified to become compatible with hydrogen fuel. The validated diesel engine model described in Section 2.1 is used for further simulations of the modified engine. To minimize the conversion costs, using consolidated components, the compression-ignition combustion system is replaced with the spark ignition, where hydrogen is delivered in the intake system via port-fuel injection (PFI). A different turbocharger is adopted due to the different air and exhaust mass flow rates. The hydrogen engine operates at the stoichiometric air/fuel ratio ($\lambda = 1$) to reach the maximum power at full load. Maximum allowed cylinder (during the combustion phase) and boost pressures are kept similar to the diesel configuration to avoid the increase in mechanical and thermal stresses. Table 3 summarizes the main modifications required to convert the diesel engine to operate with hydrogen fuel.

Table 3. Main modifications of the engine to be adequate for H_2 fueling.

Parameter	Diesel Engine	Hydrogen Engine
Fuel injection system	Direct injection	Port injection
Ignition system	Compression ignition	Spark ignition
Compression ratio [-]	18:1	12:1
Air metering	Turbocharger (turbine diameter: 89.5 mm)	Turbocharger (turbine diameter: 70 mm)
Relative air/fuel ratio (λ) at rated power	1.5	1.0

2.3. Well-to-Wheel Analysis

The process-based Life Cycle Assessment (LCA) method is one of the most analytical methods for evaluating the environmental profile of products (goods and services). LCA is regulated according to the principles defined in ISO 14040 and 14044 [22,23]. According to the application of LCA, different system boundaries can be considered. In transportation applications, a Well-to-Wheel (WTW) analysis is a common system boundary. Within the WTW analysis, the life cycle of a fuel is considered from its production up to its conversion into power at wheels. In this type of analysis, the impacts generated by the manufacturing of the transportation means (vehicle) are not included. In this study, only small modifications are applied to the engine; therefore, the diesel and H_2 trains are almost similar. In this case, a comparison based on WTW analysis becomes more relevant. The WTW emission of diesel used for transportation purposes in Europe is 89 g CO_2 eq./MJ diesel, and the low heating value (LHV) is 43.2 MJ/kg diesel [24].

In the literature, several studies using the LCA methodology calculated the Global Warming Potential (GWP) or the so-called carbon footprint of green H_2. The GWP values for PV-based H_2 via electrolysis can vary from 2.1 to 9.37 kg CO_2 eq./kg H_2 as a function of location, PV panel efficiency, and the database used [25]. The H_2 obtained through wind-powered electrolysis shows a lower carbon footprint compared to PV-based H_2 with a mean value equal to 1.29 kg CO_2 eq./kg H_2 [26]. Kolahchian et al. [25] estimated the carbon footprint of the production of PV-based H_2, taking into account the advancement of the PV industry and the current supply chain of PV panels in the Italian context. They compared their updated GWP values with the default values from the ecoinvent database [27,28]. They concluded that the ecoinvent database could not represent the carbon footprint of the production of green H_2 when state-of-the-art PV modules power the electrolysis system. Based on the real PV electricity production equivalent hours, calculated using the data from the Italian electricity transmission operator (Terna) [29], the GWP of the production of PV-based H_2 is 2.15 kg CO_2 eq./kg H_2. The annual potential of renewable electricity generation (PV, onshore and offshore wind, hydro, and geothermal) is around 715 TWh in Italy, where the majority, 50%, can be generated by PV systems [30]. Therefore, the choice of using PV-based H_2 can be justified. Also, blue hydrogen can play an important role during the transition period to a fully green H_2 market. The carbon footprint of blue H_2 for 1.85%

methane leakage and 90% carbon capture efficiency is around 3.5 kg CO_2 eq./kg H_2 (this value is calculated by averaging the results in Romano et al. [31]). Analyzing the impact of the origin of blue H_2 on the final GWP value of the train trip, a sensitivity analysis of the methane leakage rate in the gas supply chain is carried out.

Hydrogen should be compressed to increase its volume-based energy density, leading to a reduction in the storage size. The high-pressure storage for mobility applications offers pressures equal to 350 or 700 bars. In this work, hydrogen storage is assumed to be at 700 bars. Therefore, the produced hydrogen is compressed to pressures higher than the storage pressure, e.g., 800 bars. The energy requirement of the hydrogen multi-stage compression for reaching 800 bars is around 12% of hydrogen high-heating value (HHV), which means an additional power consumption equal to 4.7 kWh electricity/kg H_2 is needed [32,33]. Some studies reported an H_2 compression power consumption rate of less than 2 kWh/kg H_2 [34,35]. A manufacturer offers compressors with a power consumption of 2.7 kWh/kg H_2 for output pressures of up to 1000 bars [36]. In this work, the H_2 compression power requirement is assumed to be equal to 4 kWh/kg H_2 as an average value among the literature and manufacturer data. The Italian grid electricity with a carbon intensity of 0.371 kg CO_2 eq./kWh is considered for powering the compressors [37]. Also, for green H_2, the compression process powered by PV electricity is considered. The carbon footprint of PV electricity is extracted directly from the ecoinvent 3.5 database (cut-off method) using the default value for Italy (570 kWp open ground installation, multi-Si). Table 4 reports a summary of values considered within the Well-to-Wheel analysis.

Table 4. A summary of values considered in Well-to-Wheel analysis.

Parameter	Description
GWP of green H_2 [kg CO_2 eq./kg H_2]	2.15
GWP of blue H_2 [kg CO_2 eq./kg H_2]	3.5
GWP of diesel [kg CO_2 eq./kg Diesel]	3.85
GWP of Italian grid electricity [kg CO_2 eq./kWh]	0.371
GWP of PV electricity for Italy [kg CO_2 eq./kWh]	0.073
Storage pressure [bar]	700
Compressor power consumption [kWh/kg H_2]	4

3. Results and Discussion

The performance of the modified diesel engine fueled with hydrogen is analyzed and compared to the baseline diesel engine in Section 3.1. The consumption of both the baseline and modified diesel engine using the journey simulation is reported in Section 3.2. The results of the Well-to-Wheel analysis are presented in Section 3.3.

3.1. Performance of Modified Diesel Engine (Hydrogen-Fueled Engine)

The predicted performance of the modified diesel engine (hydrogen-fueled engine) is illustrated in Figure 4. According to the simulation results, the estimated performance of the hydrogen-fueled engine is sufficient to operate the railway vehicle, despite delivering a reduced amount of power compared to the original diesel engine. The performance reduction of the hydrogen-fueled engine is related to several factors:

- Reduced volumetric efficiency due to hydrogen PFI injection. The higher specific volume of hydrogen reduces the amount of air that can be trapped inside the cylinder, resulting in a reduction in the engine power compared to the diesel configuration.
- Lower compression ratio during engine operation to reduce knock risks. This factor clearly affects the efficiency and the maximum achievable power.
- Limited boost pressure. The reduced airflow rate restricts the increase in the boost pressure to achieve the same power as the original engine.

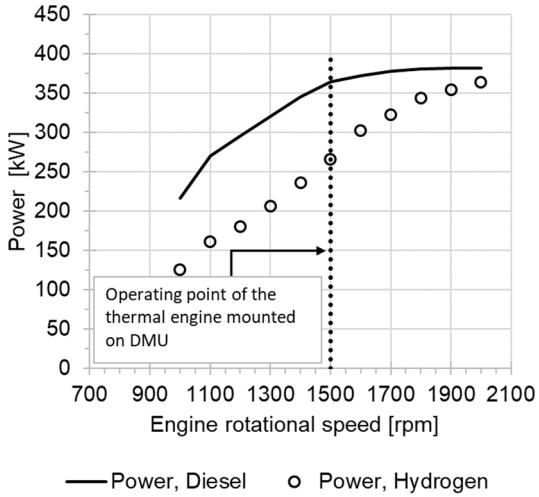

Figure 4. Comparison between the predicted effective power of the diesel and hydrogen engines at full-load operating points (the operating point of the thermal engine mounted on DMU is specified).

A more sophisticated and expensive upgrade, like the use of a direct high-pressure injection fuel system, is needed to achieve the previous level of power, leading to a rise in the total transformation costs [38,39]. Figure 5 shows the comparison between the fuel consumption of hydrogen and diesel engines as a function of engine rotational speed at full-load operating points. The mass-based hydrogen consumption is significantly lower than the diesel consumption. The notable difference between the two fuels is caused by the higher LHV of the hydrogen fuel compared to diesel fuel.

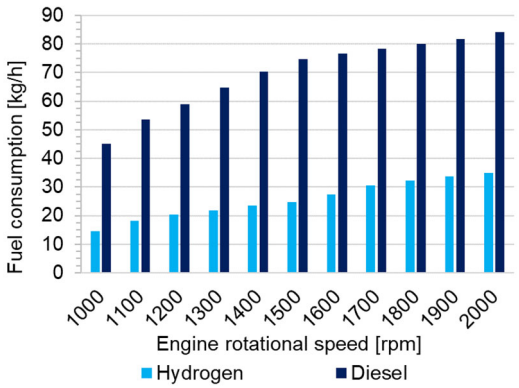

Figure 5. Comparison between predicted fuel consumption of hydrogen and diesel engines at full-load operating points.

Similar modifications applied to diesel engines to become compatible with natural gas are needed to obtain the hydrogen-fueled engine. However, the use of hydrogen entails higher costs for the injection system, as it must guarantee higher safety standards to avoid leaks and fires. According to the literature, the cost of the conversion of a diesel engine to become compatible with natural gas is in the range of EUR 8000 to EUR 12,000 for each engine [40]. The estimated cost includes the following stages:

- Engine disassembly;
- Revision and eventual replacement of some components;
- Replacement of pistons to reduce the compression ratio;
- Modification of the cylinder head to place the spark plugs;
- Installation of the phase sensor on the camshaft;
- Engine assembly;
- Installation of throttle valve for load control, ignition system, port-fuel injection system;

- Replacement of the turbocharger unit;
- New engine calibration.

Further costs are necessary for changing the after-treatment system required to reduce NO_x emissions, updating the onboard safety systems, and installing high-pressure hydrogen tanks. The cost of a high-pressure hydrogen tank for storage at 700 bars is about 15 EUR/kWh (referred to the H_2 LHV) [41].

3.2. Train Round-Trip Consumption

Several simulations of a typical mission profile of the railway vehicle under investigation are conducted for both the diesel engine and hydrogen-fueled engine configurations. The altitude profile of the railway line under investigation, as a function of the distance from its departure station up to the arrival destination, is shown in Figure 6. The red vertical lines denote the intermediate stops.

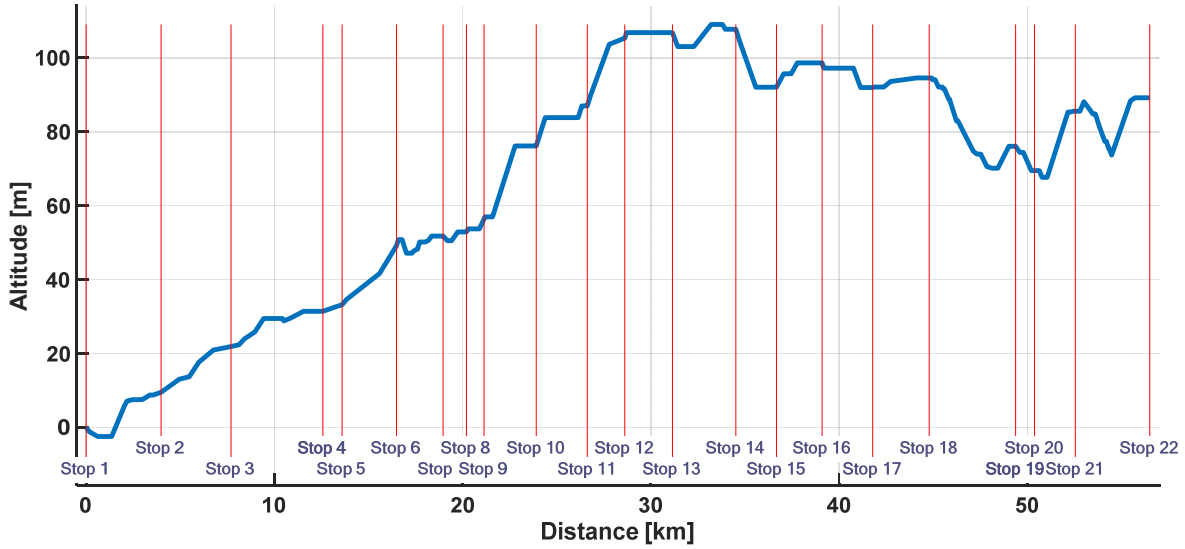

Figure 6. The altitude profile of the railway line under investigation (intermediate stops are denoted by red vertical lines).

In the baseline scenario, when the engine works with diesel, the simultaneous contribution of two onboard thermal engines can satisfy the 600 kW power request for the traction of the articulated railway vehicle. Meanwhile, the torque and speed of the electric motors are managed by inverters. This setup allows for the torque and rotational speed of the thermal unit to remain independent of the electric traction motor's performance. For the baseline diesel engine, according to Figure 2, the starting tractive force and the train base speed are 80 kN and 27 km/h, respectively. Using Equation (1), the mean fuel consumption for the railway vehicle traveling along the line under investigation is 1.11 kg/km, resulting in a round-trip diesel consumption equal to 127 kg.

As stated in Section 3.1, the hydrogen-fueled engine performs inferiorly compared to the original diesel unit, resulting in a power loss of about 100 kW. Figure 7 shows the new mechanical characteristics of the rail vehicle with hydrogen engines. Due to the lower performance of the hydrogen-fueled engine, the same railway vehicle has only 400 kW available for traction power instead of the original 600 kW.

Figure 8 compares the mechanical characteristics of a DMU in diesel and hydrogen configurations. For both the diesel and hydrogen versions, the motor drive can deliver the maximum starting tractive force. In the hydrogen version, having less power, the tractive force decreases at a lower speed, but for a suburban DMU, this did not prove to be a very penalizing factor. Figure 8 also illustrates that during the acceleration phase, the ICE operates for a large part of its characteristic curve at a constant power at the optimal

operating point as the torque and speed parameters at the wheels are controlled by the electric motor drives.

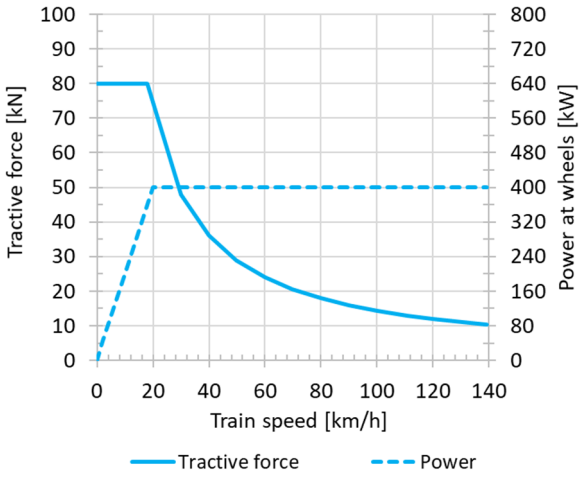

Figure 7. Tractive force (mechanical characteristic) and wheel power as a function of train speed when hydrogen thermal units work on the train.

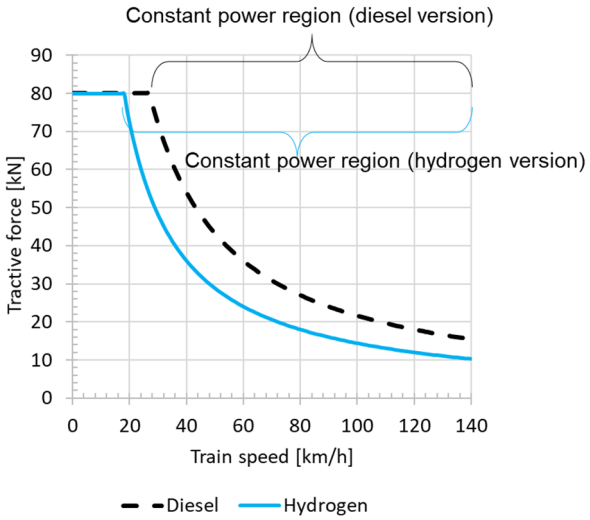

Figure 8. Mechanical characteristics for a DMU in diesel and hydrogen configurations.

Despite the reduced power of the hydrogen-fueled engine, the electric traction motors can still provide the maximum starting torque. Therefore, according to the simulation of the investigated suburban railway line equipped with the hydrogen-fueled engine, the traveling time does not increase substantially compared to the diesel engine scenario. The trip duration of the hydrogen train is predicted to be 5 min longer than the 100 min total travel time of the diesel version. The low permissible speeds and the proximity between the stops grant the limited time increase while, in the case of railway lines characterized by higher speeds and heavier rolling stokes like freight trains, performance problems might arise.

Based on the obtained mechanical characteristics curves of the hydrogen-fueled engine and assuming a similar onboard ancillary power requirement to the diesel train version, the performance of the hydrogen train along the same mission profile is predicted. The specific fuel consumption of the hydrogen engine for the operating point under consideration is equal to 90 g H_2/kWh. The simulation of the round trip of the train journey results in an overall hydrogen consumption of 87.7 kg, showing a 30% lower mass-based fuel consumption compared to the diesel version. Based on the LHV of the diesel and hydrogen,

the energy content of the diesel consumed during a round trip is around 1500 kWh, which almost doubles and reaches around 2900 kWh for the hydrogen-fueled engine. This apparently high value of total hydrogen consumption compared to the diesel case (in terms of energy content) is due to the considerable difference in maximum power (about 200 kW lower for hydrogen-fueled engine), imposing the hydrogen version to run at the maximum power for a longer time in order to guarantee a nearly identical total trip time of the investigated mission profile.

3.3. Carbon Footprint

The carbon footprint of the train fueled with diesel, green, or blue H_2 is plotted in Figure 9. When diesel is used as the train's fuel, the WTW analysis shows a GWP value equal to 4.27 kg CO_2 eq./km. Green H_2 produced and compressed via PV electricity reduces the carbon footprint to 1.87 kg CO_2 eq./km, equivalent to a 56% decrease compared to the diesel train. Compressing the PV-based H_2 with the Italian grid electricity increases the GWP value to 2.79 kg CO_2 eq./km, corresponding to a 35% reduction compared to the conventional diesel train or a 48% increase with respect to the PV-based compression scenario. The latter point emphasizes the considerable GWP impact generated at the H_2 compression stage using the grid electricity. According to the assumptions made for blue H_2 in this work, the carbon mitigation in this scenario is minimized compared to the diesel-based train. The equivalent carbon emission of the train fueled with blue H_2 is almost 3.8 kg CO_2 eq. for each kilometer (only 11% less than the diesel-based train). The blue H_2 produced under a gas supply chain with a lower methane leakage like 0.2% (GWP = 1.7 kg CO_2 eq./kg H_2) can further reduce the train's carbon footprint to 2.44 kg CO_2 eq./km (43% lower than diesel), which even overperforms the green H_2 compressed by the Italian grid electricity. However, if blue H_2 is produced under the 3.5% methane leakage rate (GWP = 5.35 kg CO_2 eq./kg H_2), the advantage of a lower GWP associated with using hydrogen disappears, and the train emits 5.2 kg CO_2 eq./km (22% higher than diesel). The sensitivity analysis on the methane leakage rate for blue H_2 is depicted with an orange dashed rectangle.

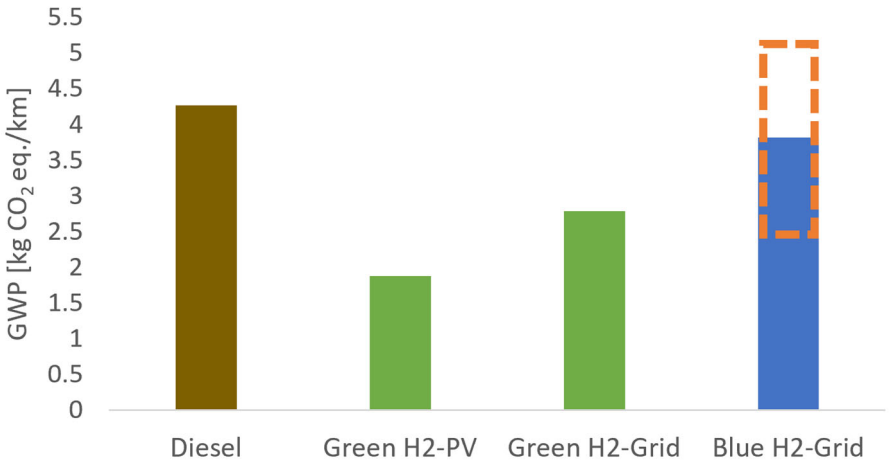

Figure 9. The GWP impact of the use phase of the studied train for different fuels per kilometer.

Figure 10 shows the GWP impact of the round trip of the train fueled with diesel or hydrogen. On each round trip, the conventional train results in a carbon footprint equal to 488 kg CO_2 eq. Utilizing hydrogen instead of diesel can bring a considerable amount of avoided emission, specifically in the case of the green H_2 powered and compressed via PV electricity. Compared to the diesel train, by using PV-based H_2, almost 274 or 170 kg CO_2 eq. is avoided for the PV or grid-compressed H_2, respectively. The average scenario for blue H_2 can result in a reduction of 52 kg CO_2 eq. for each train round trip. These reductions in equivalent CO_2 emissions suggest that carbon mitigation ranging from

56 to 11% can be obtained if diesel is substituted with hydrogen in a moderately modified diesel engine. Despite a considerable increase in the energy consumption of the hydrogen-fueled engine on a real train mission profile, the obtained reductions in equivalent CO_2 are promising, suggesting that moderately modified engines are viable candidates for decarbonizing railway sections that are not feasibly electrified.

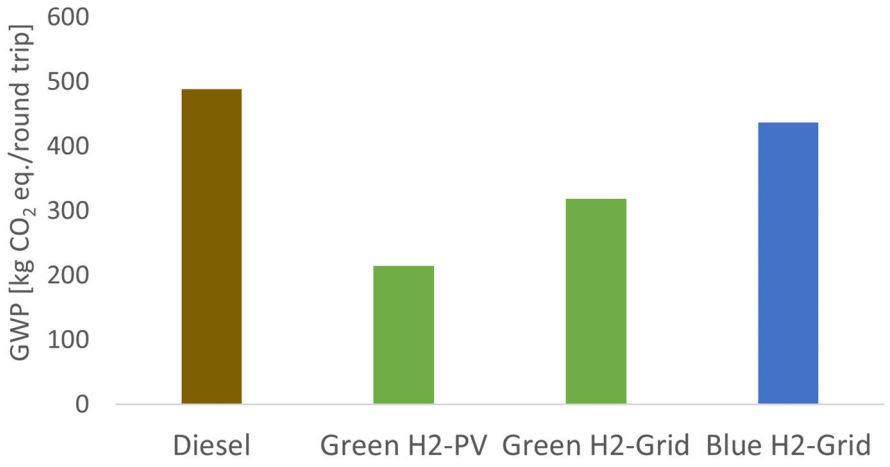

Figure 10. The GWP impact of the use phase of the studied train for different fuels for the round trip.

4. Conclusions

This paper demonstrates the potential of converting the internal combustion engines of a diesel–electric self-propelled train from diesel power to hydrogen power. A real single-decker articulated railway vehicle (Diesel Multiple Unit) currently operating on several non-electrified European railway lines is considered. This train is characterized by two or more diesel generator sets supplying power to the electric traction motors and onboard auxiliary services. The diesel engine is moderately modified to restrict the costs arising. A spark ignition system with hydrogen delivery in the intake system via port-fuel injection is utilized instead of the compression ignition combustion system. The turbocharger is replaced to handle different air and exhaust mass flow rates of the hydrogen-fueled engine. The baseline diesel engine is simulated using the Gasdyn code, and the model is validated through the measured performance values. The hydrogen-fueled engine is analyzed using the modified numerical model for spark ignition engines. Life Cycle Assessment analysis with a Well-to-Wheel system boundary is applied to evaluate the carbon footprint of the hydrogen train using both green and blue hydrogen. The main findings of this work are summarized in the following points:

- Switching the fuel from diesel to hydrogen causes a reduction in the power generated by the internal combustion engines while the electric traction motors still provide the maximum starting torque. The traction power of 600 kW for the original diesel engine is reduced to 400 kW for the modified engine working with hydrogen.
- In the case of the studied real railway line for suburban services, travel duration slightly increases from the initial 100 to 105 min for the hydrogen version. The low permissible speeds and the proximity between stops help to limit the time increase. However, for lines characterized by higher speeds and heavier rolling stokes, such as freight trains, performance problems might arise.
- The fuel consumption changes from 127 kg of diesel to 87.7 kg of hydrogen for the round trip of the mission profile. The considerable increase in the energy content of the requested fuel for the hydrogen engine is rooted in the engine's lower maximum power, forcing the hydrogen engine to run at the maximum power for a longer period to achieve nearly the same journey time as the baseline diesel engine.
- The Life Cycle Assessment analysis under a Well-to-Wheel system boundary shows that the carbon footprint of the studied train can significantly drop by utilizing low-

carbon hydrogen. Photovoltaic-based green hydrogen can reduce the equivalent CO_2 emissions by up to 56% compared to the conventional diesel train. Considering the optimistic methane leakage rate and the carbon capture efficiency for blue hydrogen production, the carbon footprint can decrease by up to 43% with respect to the baseline diesel train.

Evidencing the promising Global Warming Potential values by using low-carbon hydrogen in trains, the moderately modified engines can become a favorable candidate for decarbonizing non-feasibly or conveniently electrified railway sections.

Author Contributions: Conceptualization, D.B., T.L. and M.B.; Methodology, T.C., D.B. and T.L.; Software, M.K.T. and T.C.; Investigation, M.K.T. and T.C.; Data curation, M.K.T.; Writing—original draft, M.K.T. and T.C.; Writing—review & editing, D.B., T.L. and M.B.; Supervision, D.B., T.L. and M.B. All authors have read and agreed to the published version of the manuscript.

Funding: This research received no external funding.

Data Availability Statement: Data are contained within the article.

Conflicts of Interest: The authors declare no conflict of interest.

References

1. International Energy Agency (IEA). *World Energy Outlook 2022*; International Energy Agency (IEA): Paris, France, 2022.
2. International Energy Agency (IEA). *Global Hydrogen Review 2023*; International Energy Agency (IEA): Paris, France, 2023.
3. Bonalumi, D.; Kolahchian Tabrizi, M. Re-Evaluation of the Global Warming Potential for the Production of Lithium-Ion Batteries with Nickel–Manganese–Cobalt Cathode Chemistries in China. *Energy Fuels* **2022**, *36*, 13753–13767. [CrossRef]
4. Kolahchian Tabrizi, M.; Bonalumi, D.; Lozza, G.G. Analyzing the Global Warming Potential of the Production and Utilization of Lithium-Ion Batteries with Nickel-Manganese-Cobalt Cathode Chemistries in European Gigafactories. *Energy* **2024**, *288*, 129622. [CrossRef]
5. Liu, F.; Mauzerall, D.L.; Zhao, F.; Hao, H. Deployment of Fuel Cell Vehicles in China: Greenhouse Gas Emission Reductions from Converting the Heavy-Duty Truck Fleet from Diesel and Natural Gas to Hydrogen. *Int. J. Hydrogen Energy* **2021**, *46*, 17982–17997. [CrossRef]
6. Haseli, Y.; Naterer, G.; Dincer, I. Comparative Assessment of Greenhouse Gas Mitigation of Hydrogen Passenger Trains. *Int. J. Hydrogen Energy* **2008**, *33*, 1788–1796. [CrossRef]
7. Piraino, F.; Genovese, M.; Fragiacomo, P. Towards a New Mobility Concept for Regional Trains and Hydrogen Infrastructure. *Energy Convers. Manag.* **2021**, *228*, 113650. [CrossRef]
8. Jafari Kaleybar, H.; Brenna, M.; Li, H.; Zaninelli, D. Fuel Cell Hybrid Locomotive with Modified Fuzzy Logic Based Energy Management System. *Sustainability* **2022**, *14*, 8336. [CrossRef]
9. Brenna, M.; Foiadelli, F.; Longo, M.; Zaninelli, D. Use of Fuel Cell Generators for Cell-Propelled Trains Renovation. In Proceedings of the 2018 IEEE International Conference on Environment and Electrical Engineering and 2018 IEEE Industrial and Commercial Power Systems Europe (EEEIC/I&CPS Europe), Palermo, Italy, 12–15 June 2018; pp. 1–5.
10. Bartolucci, L.; Cordiner, S.; Mulone, V.; Pasqualini, F.; Wancura, H. A H_2 Based Retrofit of Diesel Locomotives for CO_2 Emission Reductions: Design and Control Issues. *Int. J. Hydrogen Energy* **2022**, *47*, 32669–32681. [CrossRef]
11. Nqodi, A.; Mosetlhe, T.C.; Yusuff, A.A. Advances in Hydrogen-Powered Trains: A Brief Report. *Energies* **2023**, *16*, 6715. [CrossRef]
12. Montenegro, G.; Onorati, A.; Della Torre, A. The Prediction of Silencer Acoustical Performances by 1D, 1D–3D and Quasi-3D Non-Linear Approaches. *Comput. Fluids* **2013**, *71*, 208–223. [CrossRef]
13. Cornolti, L.; Onorati, A.; Cerri, T.; Montenegro, G.; Piscaglia, F. 1D Simulation of a Turbocharged Diesel Engine with Comparison of Short and Long EGR Route Solutions. *Appl. Energy* **2013**, *111*, 1–15. [CrossRef]
14. D'Errico, G.; Ferrari, G.; Onorati, A.; Cerri, T. Modeling the Pollutant Emissions from a S.I. Engine. *SAE Trans.* **2002**, *111*, 1–11.
15. D'Errico, G.; Onorati, A.; Ellgas, S. 1D Thermo-Fluid Dynamic Modelling of an S.I. Single-Cylinder H_2 Engine with Cryogenic Port Injection. *Int. J. Hydrogen Energy* **2008**, *33*, 5829–5841. [CrossRef]
16. D'Errico, G.; Cerri, T.; Lucchini, T. *Development and Application of S.I. Combustion Models for Emissions Prediction*; SAE Technical: Warrendale, PA, USA, 2006. [CrossRef]
17. Gascón, L.; Corberán, J.M. Construction of Second-Order TVD Schemes for Nonhomogeneous Hyperbolic Conservation Laws. *J. Comput. Phys.* **2001**, *172*, 261–297. [CrossRef]
18. Winterbone, D.E.; Pearson, R.J. *Theory of Engine Manifold Design*; Society of Automotive Engineers: Warrendale, PA, USA, 2000.
19. Gasdyn Software 2023. Theory Manual. Available online: https://www.polilink.polimi.it/en/casi-di-successo/gasdyn-software-2/ (accessed on 10 November 2023).
20. Lipatnikov, A.N.; Chomiak, J. Turbulent Flame Speed and Thickness: Phenomenology, Evaluation, and Application in Multi-Dimensional Simulations. *Prog. Energy Combust. Sci.* **2002**, *28*, 1–74. [CrossRef]

21. Heywood, J.B. *Internal Combustion Engine Fundamentals*; McGraw-Hill Education: New York, NY, USA, 2018; ISBN 1260116107.
22. *ISO 14040:2006*; Environmental Management—Life Cycle Assessment—Principles and Framework. International Organization for Standardization: Geneva, Switzerland, 2006.
23. *ISO 14044:2006*; Environmental Management—Life Cycle Assessment—Requirements and Guidelines. International Organization for Standardization: Geneva, Switzerland, 2006. Available online: https://www.iso.org/standard/38498.html (accessed on 5 July 2022).
24. Eriksson, M.; Ahlgren, S. *LCAs of Petrol and Diesel: A Literature Review*; Rapport (Institutionen för Energi Och Teknik, SLU): Uppsala, Sweden, 2013.
25. Kolahchian Tabrizi, M.; Famiglietti, J.; Bonalumi, D.; Campanari, S. The Carbon Footprint of Hydrogen Produced with State-of-the-Art Photovoltaic Electricity Using Life-Cycle Assessment Methodology. *Energies* **2023**, *16*, 5190. [CrossRef]
26. Cho, H.H.; Strezov, V.; Evans, T.J. A Review on Global Warming Potential, Challenges and Opportunities of Renewable Hydrogen Production Technologies. *Sustain. Mater. Technol.* **2023**, *35*, e00567. [CrossRef]
27. Jungbluth, N.; Stucki, M.; Frischknecht, R.; Buesser, S. *Photovoltaics, Ecoinvent Report No. 6 XII*; ESU-Services Ltd.: Uster, Switzerland, 2009.
28. Wernet, G.; Bauer, C.; Steubing, B.; Reinhard, J.; Moreno-Ruiz, E.; Weidema, B. The Ecoinvent Database Version 3 (Part I): Overview and Methodology. *Int. J. Life Cycle Assess.* **2016**, *21*, 1218–1230. [CrossRef]
29. Terna Electricity Data Archives and the Latest Electricity Report. Available online: https://www.terna.it/it/sistema-elettrico/statistiche/pubblicazioni-statistiche (accessed on 10 February 2023).
30. Colbertaldo, P.; Parolin, F.; Campanari, S. A Comprehensive Multi-Node Multi-Vector Multi-Sector Modelling Framework to Investigate Integrated Energy Systems and Assess Decarbonisation Needs. *Energy Convers. Manag.* **2023**, *291*, 117168. [CrossRef]
31. Romano, M.C.; Antonini, C.; Bardow, A.; Bertsch, V.; Brandon, N.P.; Brouwer, J.; Campanari, S.; Crema, L.; Dodds, P.E.; Gardarsdottir, S.; et al. Comment on "How Green Is Blue Hydrogen?". *Energy Sci. Eng.* **2022**, *10*, 1944–1954. [CrossRef]
32. Makridis, S.S. Hydrogen Storage and Compression. In *Methane and Hydrogen for Energy Storage*; Institution of Engineering and Technology: Stevenage, UK, 2016; pp. 1–28.
33. Tahan, M.-R. Recent Advances in Hydrogen Compressors for Use in Large-Scale Renewable Energy Integration. *Int. J. Hydrogen Energy* **2022**, *47*, 35275–35292. [CrossRef]
34. Zhang, J.Z.; Li, J.; Li, Y.; Zhao, Y. Established Methods Based on Compression and Cryogenics. In *Hydrogen Generation, Storage, and Utilization*; Wiley: Hoboken, NJ, USA, 2014; pp. 75–90.
35. Valente, A.; Iribarren, D.; Candelaresi, D.; Spazzafumo, G.; Dufour, J. Using Harmonised Life-Cycle Indicators to Explore the Role of Hydrogen in the Environmental Performance of Fuel Cell Electric Vehicles. *Int. J. Hydrogen Energy* **2020**, *45*, 25758–25765. [CrossRef]
36. Linde, A.G. The Ionic Compressor IC90 (90 MPa). Available online: https://www.boconline.co.uk/en/images/Datasheet_Ionic%20Fueler%20IC90_tcm410-410855.pdf (accessed on 10 December 2023).
37. Scarlat, N.; Prussi, M.; Padella, M. Quantification of the Carbon Intensity of Electricity Produced and Used in Europe. *Appl. Energy* **2022**, *305*, 117901. [CrossRef]
38. Munshi, S.; Garner, G.; Theissl, H.; Hofer, F.; Raser, B. Total Cost of Ownership (TCO) Analysis for Heavy Duty Hydrogen Fueled Powertrains. Available online: https://www.avl.com/documents/10138/2703324/20201225_Westport_AVL_Whitepaper_Hydrogen_HPDI_final.pdf/3f482167-d9ee-8a00-7e3a-ceb024373fe9 (accessed on 4 May 2021).
39. Jin, S.; Li, J.; Deng, L.; Wu, B. Effect of the HPDI and PPCI Combustion Modes of Direct-Injection Natural Gas Engine on Combustion and Emissions. *Energies* **2021**, *14*, 1957. [CrossRef]
40. Green Car Congress Omnitek Develops Diesel-to-Natural Gas Engine Conversion Kits for Mercedes OM904/OM906. Available online: https://www.greencarcongress.com/2012/04/omnitek-20120419.html (accessed on 20 December 2023).
41. James, B.D.; Houchins, C.; Huya-Kouadio, J.M.; DeSantis, D.A. *Final Report: Hydrogen Storage System Cost Analysis*; Strategic Analysis Inc.: Arlington, VA, USA, 2016.